10174 *Inorg. Chem.* **2010**, *49*, 10174–10182
DOI: 10.1021/ic101451y

Inorganic Chemistry
Article

Synthetic and Structural Investigations of Linear and Macrocyclic Nickel/Iron/Sulfur Cluster Complexes

Li-Cheng Song,* Yu-Long Li, Ling Li, Zhen-Chao Gu, and Qing-Mei Hu

Department of Chemistry, State Key Laboratory of Elemento-Organic Chemistry, Nankai University, Tianjin 300071, China

Received July 21, 2010

Three series of new Ni/Fe/S cluster complexes have been prepared and structurally characterized. One series of such complexes includes the linear type of (diphosphine)Ni-bridged double-butterfly Fe/S complexes $[(\mu\text{-RS})(\mu\text{-S=CS})Fe_2(CO)_6]_2[Ni(diphosphine)]$ (**1**−**6**; R = Et, *t*-Bu, *n*-Bu, Ph; diphosphine = dppv, dppe, dppb), which were prepared by reactions of monoanions $[(\mu\text{-RS})(\mu\text{-CO})Fe_2(CO)_6]^-$ (generated in situ from $Fe_3(CO)_{12}$, Et_3N, and RSH) with excess CS_2, followed by treatment of the resulting monoanions $[(\mu\text{-RS})(\mu\text{-S=CS})Fe_2(CO)_6]^-$with (diphosphine)$NiCl_2$. The second series consists of the macrocyclic type of (diphosphine)Ni-bridged double-butterfly Fe/S complexes $[\mu\text{-S}(CH_2)_4S\text{-}\mu][(\mu\text{-S=CS})Fe_2(CO)_6]_2[Ni(diphosphine)]$ (**7**−**9**; diphosphine = dppv, dppe, dppb), which were produced by the reaction of dianion $[\{\mu\text{-S}(CH_2)_4S\text{-}\mu\}\{(\mu\text{-CO})Fe_2(CO)_6\}_2]^{2-}$ (formed in situ from $Fe_3(CO)_{12}$, Et_3N, and dithiol $HS(CH_2)_4SH$ with excess CS_2, followed by treatment of the resulting dianion $[\{\mu\text{-S}(CH_2)_4S\text{-}\mu\}\{(\mu\text{-S=CS})Fe_2(CO)_6\}_2]^{2-}$ with (diphosphine)$NiCl_2$. However, more interestingly, when dithiol $HS(CH_2)_4SH$ (used for the production of **7**−**9**) was replaced by $HS(CH_2)_3SH$ (a dithiol with a shorter carbon chain), the sequential reactions afforded another type of macrocyclic Ni/Fe/S complex, namely, the (diphosphine)Ni-bridged quadruple-butterfly Fe/S complexes $[\{\mu\text{-S}(CH_2)_3S\text{-}\mu\}\{(\mu\text{-S=CS})Fe_2(CO)_6\}_2]_2[Ni(diphosphine)]_2$ (**10**−**12**; diphosphine = dppv, dppe, dppb). While a possible pathway for the production of the two types of novel metallomacrocycles **7**−**12** is suggested, all of the new complexes **1**−**12** were characterized by elemental analysis and spectroscopy and some of them by X-ray crystallography.

Introduction

In recent years, the Ni/Fe/S cluster complexes have received considerable attention, largely because of their structural diversity and novel properties and, in particular, their close relevance to [NiFe]hydrogenases ([NiFe]Hases).[1−3] [NiFe]Hases are highly effective natural enzymes that can catalyze the simplest chemical reaction, $H_2 \rightleftharpoons 2H^+ + 2e$, in a wide variety of microorganisms.[4−7] Recent X-ray crystallographic studies revealed that the active site of [NiFe]Hases consists of a butterfly [NiFe2S] cluster core, in which the Fe atom is coordinated by one terminal CO and two terminal CN^- ligands, the Ni atom is coordinated by two terminal cysteinyl (Cys−S) ligands, and the two metal centers are combined by two bridging Cys−S ligands (Figure 1).[8−11]

Under the guidance of the determined structure by X-ray crystallography, many synthetic chemists have designed and successfully prepared a variety of Ni/Fe/S complexes as

---

*To whom correspondence should be addressed. E-mail: lcsong@nankai.edu.cn.

(1) Canaguier, S.; Artero, V.; Fontecave, M. *Dalton Trans.* **2008**, 315.

(2) (a) Marr, A. C.; Spencer, D. J. E.; Schröder, M. *Coord. Chem. Rev.* **2001**, *219−221*, 1055. (b) Bouwman, E.; Reedijk, J. *Coord. Chem. Rev.* **2005**, *249*, 1555.

(3) (a) Fontecilla-Camps, J. C.; Volbeda, A.; Cavazza, C.; Nicolet, Y. *Chem. Rev.* **2007**, *107*, 4273. (b) Tard, C.; Pickett, C. J. *Chem. Rev.* **2009**, *109*, 2245.

(4) Cammack, R. *Nature* **1999**, *397*, 214.

(5) Adams, M. W. W.; Stiefel, E. I. *Science* **1998**, *282*, 1842.

(6) Frey, M. *ChemBioChem.* **2002**, *3*, 153.

(7) Vignais, P. M.; Billoud, B. *Chem. Rev.* **2007**, *107*, 4206.

(8) (a) Volbeda, A.; Charon, M. H.; Piras, C.; Hatchikian, E. C.; Frey, M.; Fontecilla-Camps, J. C. *Nature* **1995**, *373*, 580. (b) Happe, R. P.; Roseboom, W.; Pierik, A. J.; Albracht, S. P. J.; Bagley, K. A. *Nature* **1997**, *385*, 126.

(9) Volbeda, A.; Garcin, E.; Piras, C.; de Lacey, A. L.; Fernandez, V. M.; Hatchikian, E. C.; Frey, M.; Fontecilla-Camps, J. C. *J. Am. Chem. Soc.* **1996**, *118*, 12989.

(10) Fontecilla-Camps, J. C.; Frey, M.; Garcin, E.; Hatchikian, C.; Montet, Y.; Piras, C.; Vernède, X.; Volbeda, A. *Biochimie* **1997**, *79*, 661.

(11) Higuchi, Y.; Ogata, H.; Miki, K.; Yasuoka, N.; Yagi, T. *Structure* **1999**, *7*, 549.

(12) (a) Osterloh, F.; Saak, W.; Hasse, D.; Pohl, S. *Chem. Commun.* **1997**, 979. (b) Smith, M. C.; Barclay, J. E.; Cramer, S. P.; Davies, S. C.; Gu, W.-W.; Hughes, D. L.; Longhurst, S.; Evans, D. J. *J. Chem. Soc., Dalton Trans.* **2002**, 2641. (c) Lai, C. H.; Reibenspies, J. H.; Darensbourg, M. Y. *Angew. Chem., Int. Ed. Engl.* **1996**, *35*, 2390.

(13) (a) Bouwman, E.; Henderson, R. K.; Spek, A. L.; Reedijk, J. *Eur. J. Inorg. Chem.* **1999**, 217. (b) Stenson, P. A.; Marin-Becerra, A.; Wilson, C.; Blake, A. J.; McMaster, J.; Schröder, M. *Chem. Commun.* **2006**, 317. (c) Osterloh, F.; Saak, W.; Haase, D.; Pohl, S. *Chem. Commun.* **1996**, 777.

(14) (a) Zhu, W. F.; Marr, A. C.; Wang, Q.; Neese, F.; Spencer, D. J. E.; Blake, A. J.; Cooke, P. A.; Wilson, C.; Schröder, M. *Proc. Natl. Acad. Sci. U. S.A.* **2005**, *102*, 18280. (b) Wang, Q.; Barclay, J. E.; Blake, A. J.; Davies, E. S.; Evans, D. J.; Marr, A. C.; McInnes, E. J. L.; McMaster, J.; Wilson, C.; Schröder, M. *Chem.—Eur. J.* **2004**, *10*, 3384.

(15) (a) Smith, M. C.; Barclay, J. E.; Davies, S. C.; Hughes, D. L.; Evans, D. J. *Dalton Trans.* **2003**, 4147. (b) Li, Z. L.; Ohki, Y.; Tatsumi, K. *J. Am. Chem. Soc.* **2005**, *127*, 8950. (c) Sellmann, D.; Lauderbach, F.; Geipel, F.; Heinemann, F. W.; Moll, M. *Angew. Chem., Int. Ed.* **2004**, *43*, 3141.

(16) (a) Ohki, Y.; Yasumura, K.; Kuge, K.; Tanino, S.; Ando, M.; Li, Z.; Tatsumi, K. *Proc. Natl. Acad. Sci .U.S.A.* **2008**, *105*, 7652. (b) Pal, S.; Ohki, Y.; Yoshikawa, T.; Kuge, K.; Tatsumi, K. *Chem.—Asian J.* **2009**, *4*, 961. (c) Jiang, J.; Maruani, M.; Solaimanzadeh, J.; Lo, W.; Koch, S. A.; Millar, M. *Inorg. Chem.* **2009**, *48*, 6359.

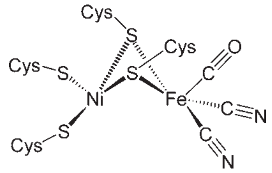

Figure 1. Structure of the active site of [NiFe]Hases.

biomimetic models for the active site of [NiFe]Hases.[12−16] As part of our projects regarding Fe/E (E = S, Se, Te) cluster chemistry[17−20] and biomimetic chemistry of hydrogenases,[21−23] we recently initiated a study on the sequential reactions of in situ prepared one-μ-CO-containing monoanion $[(\mu\text{-RS})(\mu\text{-CO})Fe_2(CO)_6]^-$[24,25] and a two-$\mu$-CO-containing dianion $[\{(\mu\text{-SZS-}\mu)\}\{(\mu\text{-CO})Fe_2(CO)_6\}_2]^{2-}$[18,19] with the electrophile CS_2 and various diphosphine-chelated $NiCl_2$ fragments. Our main purpose for this study is to prepare some new Ni/Fe/S cluster complexes that could be regarded as structural models for the active site of [NiFe]Hases. Interestingly, from the studied sequential reactions, three series of new Ni/Fe/S complexes have been successfully synthesized. One series involves the linear (diphosphine)Ni-bridged double-butterfly Fe/S cluster complexes, whereas another two series are novel metallomacrocycles including the (diphosphine)Ni-bridged double- and quadruple-butterfly Fe/S cluster complexes, respectively. Herein, we report the interesting results obtained from this study.

Results and Discussion

Synthesis and Characterization of Linear Ni-Bridged Double-Butterfy Fe/S Clusters $[(\mu\text{-RS})(\mu\text{-S=CS})Fe_2(CO)_6]_2$-[Ni(dppv)] [R = Et (1), *t*-Bu (2)], $[(\mu\text{-RS})(\mu\text{-S=CS})Fe_2(CO)_6]_2$[Ni(dppe)] [R = *n*-Bu (3), Ph (4)], and $[(\mu\text{-RS})(\mu\text{-S=CS})Fe_2(CO)_6]_2$[Ni(dppb)] [R = Et (5), *t*-Bu (6)]. We found that the linear (diphosphine)Ni-bridged double-butterfly Fe/S complexes **1**−**6** could be prepared by reactions of the $[Et_3NH]^+$ salts of one-μ-CO-containing monoanion $[(\mu\text{-RS})(\mu\text{-CO})Fe_2(CO)_6]^-$ (**A**; generated in situ from $Fe_3(CO)_{12}$, Et_3N, and RSH)[24,25] with excess CS_2, followed by treatment of the resulting $[Et_3NH]^+$ salts of one-μ-CS_2-containing monoanion $[(\mu\text{-RS})(\mu\text{-S=CS})Fe_2(CO)_6]^-$ (**A′**)[26,27] with diphosphine dppv-, dppe-, or dppb-chelated $NiCl_2$, respectively (Scheme 1).

Scheme 1

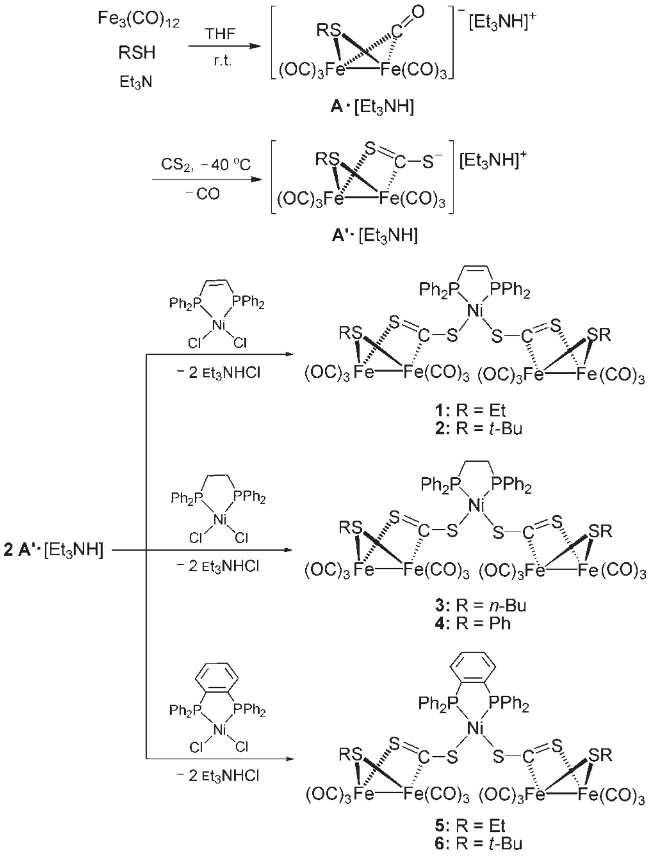

Linear Ni/Fe/S complexes **1**−**6** are air-stable red solids, which were characterized by elemental analysis and IR and ^1H and ^{31}P NMR spectroscopies. For example, the IR spectra of **1**−**6** displayed three strong absorption bands in the region 2057−1974 cm^{-1} for their terminal carbonyls and one medium absorption band in the range 989−984 cm^{-1} for their C=S groups, each bridged between two Fe atoms. Apparently, it is due to such a type of coordination that the absorption band of C=S groups in **1**−**6** is located at much lower frequencies than that of C=S groups in free CS_2 (1533 cm^{-1}). In addition, the medium band caused by the C=S groups in **1**−**6** falls within the range 1120−860 cm^{-1} exhibited by the coordinated C=S groups in some other transition-metal complexes.[27−29] The ^1H NMR spectra of **1** and **5** showed two quartets for their methylene groups at 2.37/2.58 and 2.39/2.58 ppm with an identical integration. This implies that the two ethyl groups in **1** or **5** attached to the bridged S atoms occupy the axial and equatorial positions with respect to the butterfly core,[30,31] respectively. However, in contrast to **1** and **5**, the two *t*-Bu groups in **2** or **6** displayed only one singlet at ca. 1.40 ppm, and thus they

---

(17) (a) Song, L.-C. *Trends Organomet. Chem.* **1999**, *3*, 1. (b) Song, L.-C. *Sci. China, Ser. B: Chem.* **2009**, *52*, 1. (c) Song, L.-C. *Acc. Chem. Res.* **2005**, *38*, 21.

(18) Song, L.-C.; Fan, H.-T.; Hu, Q.-M. *J. Am. Chem. Soc.* **2002**, *124*, 4566.

(19) Song, L.-C.; Fan, H.-T.; Hu, Q.-M.; Yang, Z.-Y.; Sun, Y.; Gong, F.-H. *Chem.—Eur. J.* **2003**, *9*, 170.

(20) Song, L.-C.; Zeng, G.-H.; Lou, S.-X.; Zan, H.-N.; Ming, J.-B.; Hu, Q.-M. *Organometallics* **2008**, *27*, 3714.

(21) Song, L.-C.; Tang, M.-Y.; Su, F.-H.; Hu, Q.-M. *Angew. Chem., Int. Ed.* **2006**, *45*, 1130.

(22) (a) Song, L.-C.; Yang, Z.-Y.; Bian, H.-Z.; Liu, Y.; Wang, H.-T.; Liu, X.-F.; Hu, Q.-M. *Organometallics* **2005**, *24*, 6126. (b) Song, L.-C.; Gao, W.; Feng, C.-P.; Wang, D.-F.; Hu, Q.-M. *Organometallics* **2009**, *28*, 6121.

(23) (a) Song, L.-C.; Li, C.-G.; Gao, J.; Yin, B.-S.; Luo, X.; Zhang, X.-G.; Bao, H.-L.; Hu, Q.-M. *Inorg. Chem.* **2008**, *47*, 4545. (b) Song, L.-C.; Yan, J.; Li, Y.-L.; Wang, D.-F.; Hu, Q.-M. *Inorg. Chem.* **2009**, *48*, 11376.

(24) Seyferth, D.; Womack, G. B.; Dewan, J. C. *Organometallics* **1985**, *4*, 398.

(25) Song, L.-C.; Yan, C.-G.; Hu, Q.-M.; Wang, R.-J.; Mak, T. C. W.; Huang, X.-Y. *Organometallics* **1996**, *15*, 1535.

(26) Seyferth, D.; Womack, G. B.; Archer, C. M.; Fackler, J. P., Jr.; Marler, D. O. *Organometallics* **1989**, *8*, 443.

(27) Song, L.-C.; Yan, C.-G.; Hu, Q.-M.; Wu, B.-M.; Mak, T. C. W. *Organometallics* **1997**, *16*, 632.

(28) Patin, H.; Mignani, G.; Mahé, C.; LaMarouille, J.-Y.; Southern, T. G.; Benoit, A.; Grandjean, P. *J. Organomet. Chem.* **1980**, *197*, 315.

(29) Song, L.-C.; Yan, C.-G.; Hu, Q.-M.; Wang, R.-J.; Mak, T. C. W. *Organometallics* **1995**, *14*, 5513.

(30) Seyferth, D.; Henderson, R. S.; Song, L.-C. *Organometallics* **1982**, *1*, 125.

(31) Shaver, A.; Fitzpatrick, P. J.; Steliou, K.; Butler, I. S. *J. Am. Chem. Soc.* **1979**, *101*, 1313.

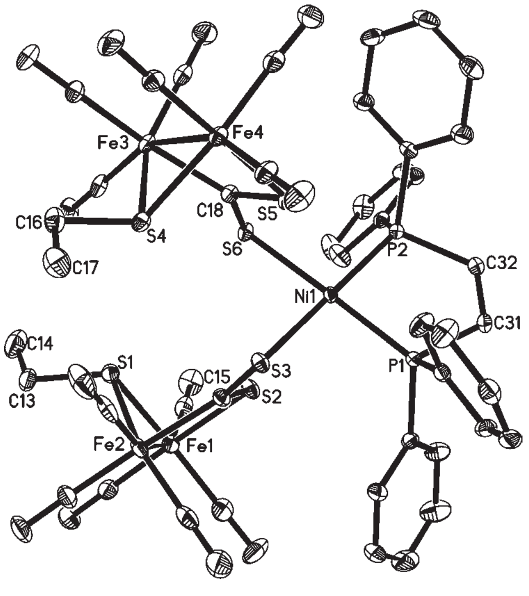

Figure 2. ORTEP view of **1** with 30% probability level ellipsoids.

are most likely attached to the bridged S atoms in the equatorial positions.[32] This has been confirmed by the crystal structure of **2** (vide infra). The ^{31}P NMR spectra of **1**−**6** exhibited a singlet at 51.62−61.83 ppm attributed to their diphosphine P atoms.

The structures of complexes **1**, **2**, **4**, and **5** were unequivocally confirmed by X-ray crystal diffraction analysis. While their molecular structures are depicted in Figures 2−5, Table 1 lists their selected bond lengths and angles. Because all complexes **1**, **2**, **4**, and **5** are isostructural, we only give a detailed description on the representive complex **1**. As can be seen in Figure 2, complex **1** indeed comprises two single-butterfly cluster moieties Fe1Fe2S1S2C15S3 and Fe3Fe4S4S5C18S6, which are combined by the dppv-chelated Ni atom through Ni1−S3 and Ni1−S6 bonds. All 12 CO′s bound to Fe atoms are terminal, and the two ethyl groups attached to S1 and S4 atoms occupy the equatorial positions (the nonbonded angle $\angle$C13−S1$\cdots$S2 = 163.38°) and C16−S4 (the nonbonded angle $\angle$C16−S4$\cdots$S5 = 164.10°). It follows that although complex **1** existed with an axial ethyl and an equatorial ethyl in a CDCl$_3$ solution during ^{1}H NMR determination, the axial ethyl was converted to the more stable equatorial ethyl during the course of single-crystal growth.[30,31] The thiocarbonyls C15=S2 (1.687 Å) and C18=S5 (1.679 Å) in complex **1**, similar to other μ-CS$_2$-containing butterfly Fe/S complexes,[27−29] are coordinated to Fe2 and Fe3 by σ bonds (Fe2−C15 = 1.968 Å; Fe3−C18 = 1.981 Å) and to Fe1 and Fe4 through donation of the lone electron pair from S2 or S5 (Fe1−S2 = 2.3036 Å, Fe4−S5 = 2.2959 Å). It is worth pointing out that, as can be seen intuitively in Figures 3−5, the two *t*-Bu groups of **2**, two phenyl groups of **4**, and two ethyl groups of **5** are attached respectively to S5/S6, S1/S6, and S1/S4 all in equatorial positions.

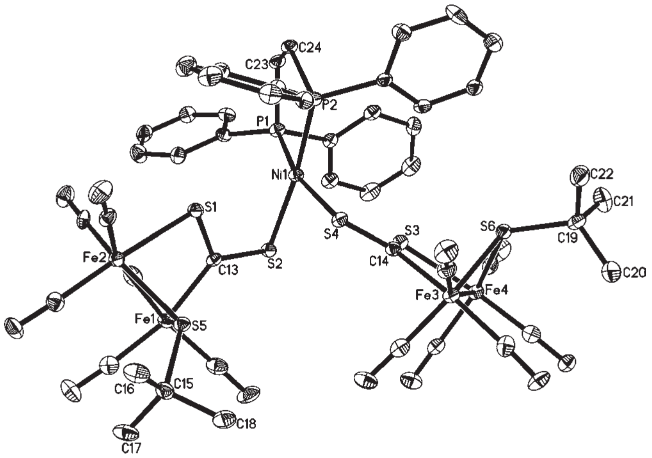

Figure 3. ORTEP view of **2** with 30% probability level ellipsoids.

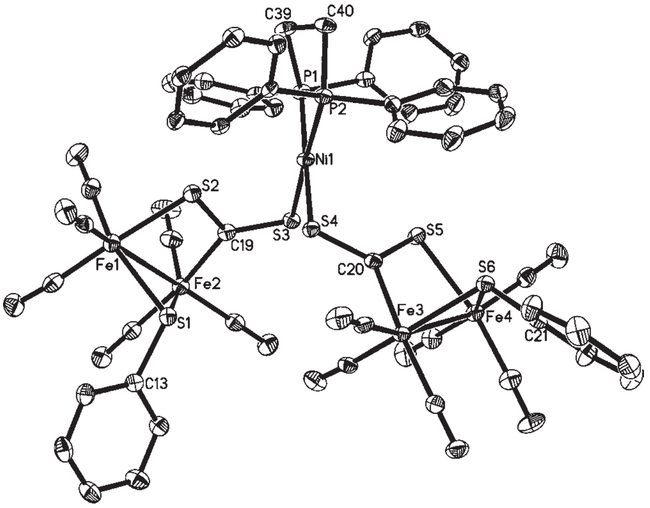

Figure 4. ORTEP view of **4** with 50% probability level ellipsoids.

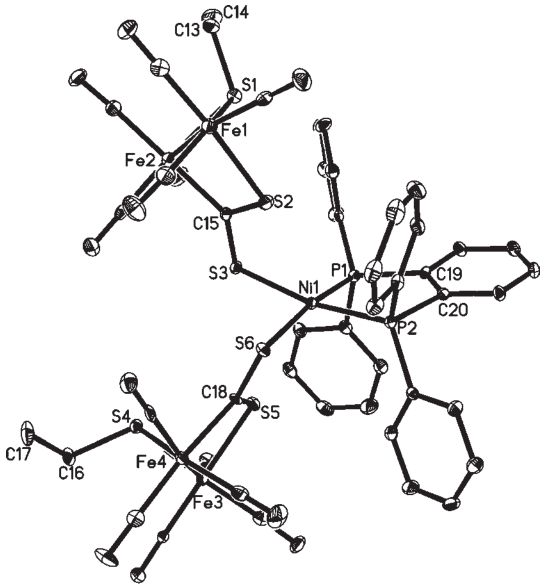

Figure 5. ORTEP view of **5** with 50% probability level ellipsoids.

Synthesis and Characterization of Macrocyclic Ni-Bridged Double-Butterfly Fe/S Clusters [μ-S(CH$_2$)$_4$S-μ][(μ-S=CS)Fe$_2$(CO)$_6$]$_2$[Ni(diphosphine)] [diphosphine = dppv (7), dppe (8), dppb (9)]. We further found that the macrocyclic (diphosphine)Ni-bridged double-butterfly Fe/S complexes **7**−**9** could be prepared by sequential reactions of the [Et$_3$NH]$^+$ salt of a two-μ-CO-containing dianion

---

[32] de Beer, J. A.; Haines, R. J. *J. Organomet. Chem.* **1970**, *24*, 757.

Table 1. Selected Bond Lengths (Å) and Angles (deg) for **1**, **2**, **4**, and **5**

	1		
Fe1−Fe2	2.6209(12)	Ni1−S3	2.2356(12)
Fe1−S1	2.2376(13)	Ni1−S6	2.2513(12)
Fe1−S2	2.3036(14)	Ni1−P2	2.1612(12)
Fe3−Fe4	2.6303(10)	Ni1−P1	2.1635(12)
S1−Fe1−S2	82.54(5)	P2−Ni1−S3	178.41(5)
S1−Fe1−Fe2	54.61(4)	P2−Ni1−S6	91.64(5)
S2−Fe1−Fe2	76.05(4)	P1−Ni1−S6	177.79(5)
S1−Fe2−Fe1	54.01(4)	S3−Ni1−S6	88.82(5)
P2−Ni1−P1	88.57(5)	P1−Ni1−S3	91.03(5)
	2		
Fe1−S5	2.261(2)	Ni1−S4	2.233(2)
Fe1−Fe2	2.6282(16)	Ni1−S2	2.246(2)
Fe2−S5	2.239(3)	Ni1−P1	2.172(2)
Fe2−S1	2.317(2)	Ni1−P2	2.171(2)
Fe2−S5−Fe1	71.46(8)	P2−Ni1−P1	87.14(9)
S5−Fe2−Fe1	54.67(6)	P1−Ni1−S4	165.11(9)
S5−Fe1−Fe2	53.87(7)	P2−Ni1−S4	88.78(9)
S5−Fe2−S1	80.94(8)	P1−Ni1−S2	94.75(9)
S1−Fe2−Fe1	76.11(6)	P2−Ni1−S2	172.09(9)
	4		
Ni1−P2	2.1792(15)	Fe1−S1	2.2650(17)
Ni1−P1	2.1839(16)	Fe2−S1	2.2602(16)
Ni1−S4	2.2298(15)	Fe1−S2	2.3089(18)
Ni1−S3	2.2423(14)	Fe1−Fe2	2.6350(13)
P2−Ni1−P1	87.69(6)	S1−Fe1−S2	82.58(6)
P2−Ni1−S4	88.81(5)	S1−Fe1−Fe2	54.30(4)
P1−Ni1−S4	176.49(6)	S1−Fe2−Fe1	54.47(4)
P2−Ni1−S3	178.07(6)	S6−Fe3−Fe4	54.51(5)
P1−Ni1−S3	93.04(5)	S6−Fe4−S5	80.12(5)
	5		
Ni1−P1	2.1642(2)	Fe2−S1	2.267(2)
Ni1−P2	2.1741(19)	Fe3−S4	2.2412(19)
Ni1−S3	2.2337(18)	Fe3−S5	2.322(2)
Ni1−S6	2.2392(19)	Fe1−Fe2	2.6286(16)
S3−Ni1−S6	90.78(7)	P1−Ni1−S3	91.00(7)
S1−Fe1−S2	82.16(7)	P2−Ni1−S3	167.55(8)
S1−Fe1−Fe2	54.83(6)	P1−Ni1−S6	169.08(8)
S2−Fe1−Fe2	76.11(6)	Fe1−S1−Fe2	71.44(7)
S1−Fe2−Fe1	53.72(6)	P1−Ni1−P2	88.01(7)

Scheme 2

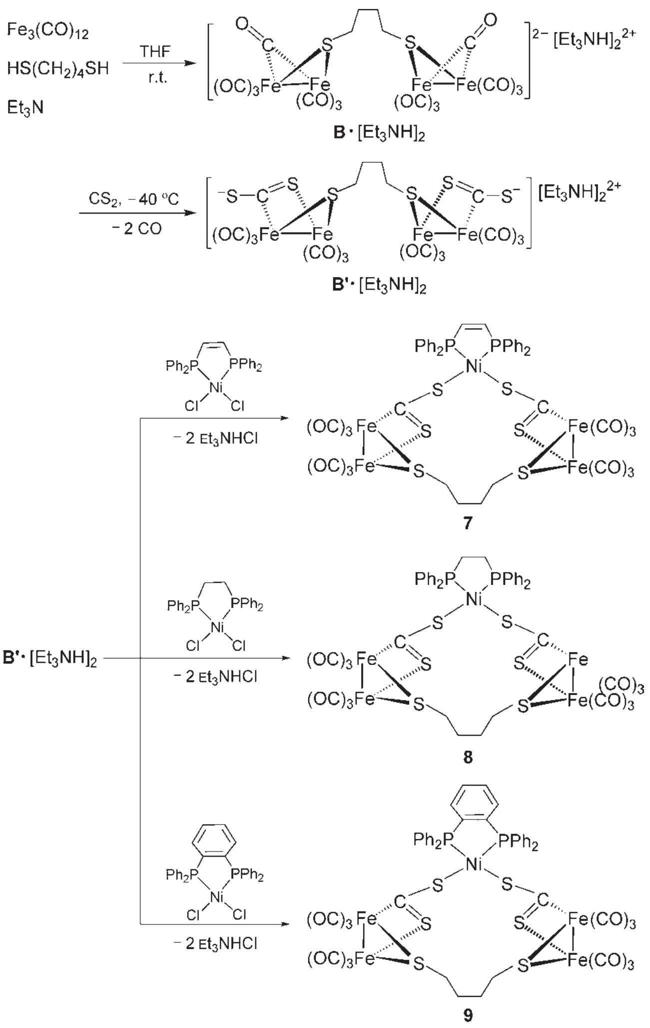

$[\{\mu\text{-S}(CH_2)_4S\text{-}\mu\}\{(\mu\text{-CO})Fe_2(CO)_6\}_2]^{2-}$ (**B**;[19] formed in situ from $Fe_3(CO)_{12}$, dithiol $HS(CH_2)_4SH$, and Et_3N) with excess CS_2, followed by treatment of the resultant $[Et_3NH]^+$ salt of two-μ-CS_2-containing dianion $[\{\mu\text{-S}(CH_2)_4S\text{-}\mu\}\{(\mu\text{-S=CS})Fe_2(CO)_6\}_2]^{2-}$ (**B′**)[19] with dppv-, dppe-, and dppb-chelated $NiCl_2$, respectively (Scheme 2).

Macrocyclic Ni/Fe/S complexes **7**−**9** are also air-stable, red solids. They have been characterized by elemental analysis and IR and ^1H and ^{31}P NMR spectroscopies. For example, similar to **1**−**6**, the IR spectra of **7**−**9** showed three absorption bands in the range 2053−1975 cm^{-1} for their terminal CO′s and one medium absorption band in the region 991−989 cm^{-1} for their C=S functionality bridged between two Fe atoms. In addition, the ^{31}P NMR spectra of **7**−**9** exhibited one singlet in the range 53.79−62.45 ppm for P atoms in their diphosphine ligands.

The molecular structure of **8** was unambiguously confirmed by X-ray crystal diffraction techniques. While its structure is presented in Figure 6, Table 2 lists their selected bond lengths and angles. Figure 6 shows that complex **8** is indeed a Ni/Fe/S macrocyclic complex, which consists of two single-butterfly cluster moieties Fe1Fe2S3S2C39S1 and Fe3Fe4S6S5C44S4 linked together by a butylene chain (via C40−S3 and C43−S6 bonds) and a dppe-chelated nickel moiety (via Ni1−S1 and Ni1−S4 bonds), respectively. This complex might be viewed as having a 17-membered metallomacrocycle NiS1C39S2Fe2Fe1S3C40C41C42C43 S6Fe4Fe3S5C44S4. In addition, all 12 carbonyls of **8** are terminal and the two coordinated thiocarbonyls C39=S2 (1.676 Å) and C44=S5 (1.691 Å) are much shorter than that of free CS_2 and comparable to those found in **1**, **2**, **4**, and **5** and other butterfly Fe/S complexes.[27−29] The butylene group is attached to S3/S6 in axial positions[30,31] (the nonbonded angles: ∠C40−S3···S2 = 77.35° and ∠C43−S6···S5 = 75.80°) in order to reduce the ring strains in such types of macrocycles. All Fe atoms of **8** adopt the expected square-pyramidal geometry with the normal Fe−Fe bond lengths (average 2.617 Å).[19,33,34] The Ni atom has a slightly distorted square-planar geometry with normal Ni−S (average 2.233 Å) and Ni−P (average 2.187 Å) bond lengths.[35−37]

---

(33) van der Vlugt, J. I.; Rauchfuss, T. B.; Wilson, S. R. *Chem.—Eur. J.* **2006**, *12*, 90.

(34) Morvan, D.; Capon, J.-F.; Gloaguen, F.; Goff, A. L.; Marchivie, M.; Michaud, F.; Schollhammer, P; Talarmin, J.; Yaouanc, J.-J.; Pichon, R.; Kervarec, N. *Organometallics* **2007**, *26*, 2042.

(35) Chalbot, M.-C.; Mills, A. M.; Spek, A. L.; Long, G. J.; Bouwman, E. *Eur. J. Inorg. Chem.* **2003**, 453.

(36) Spencer, D. J. E.; Blake, P. A.; Cooke, M.; Schröder, M. *J. Inorg. Biochem.* **1999**, *74*, 303.

(37) Davies, S. C.; Evans, D. J.; Hughes, D. L.; Longhurst, S.; Sanders, J. R. *Chem. Commun.* **1999**, 1935.

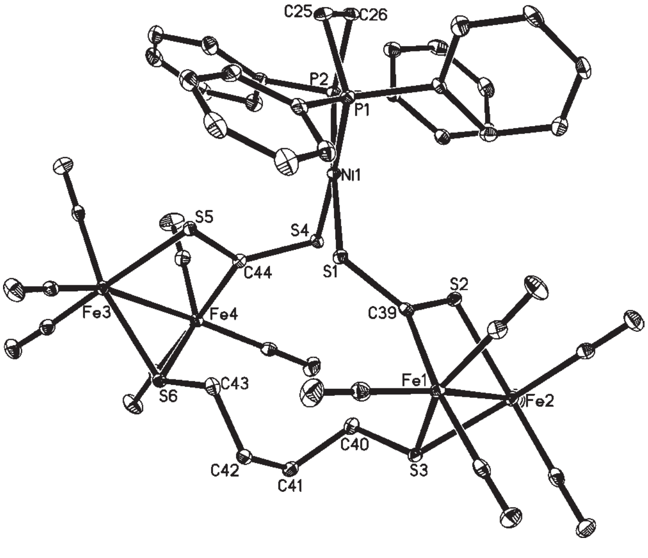

Figure 6. ORTEP view of **8** with 30% probability level ellipsoids.

Table 2. Selected Bond Lengths (Å) and Angles (deg) for **8** and **11**

		8	
Fe1−Fe2	2.6162(11)	Ni1−S1	2.2260(10)
Fe1−S3	2.2535(13)	Ni1−S4	2.2390(12)
Fe2−S3	2.2567(12)	Ni1−P2	2.1864(10)
Fe2−S2	2.3144(10)	Ni1−P1	2.1875(13)
S3−Fe1−Fe2	54.60(4)	S6−Fe3−Fe4	54.73(3)
S3−Fe2−S2	91.36(4)	P1−Ni1−S1	88.45(4)
S3−Fe2−Fe1	54.49(3)	P2−Ni1−S4	90.32(4)
S2−Fe2−Fe1	75.27(4)	P2−Ni1−P1	87.32(4)
S6−Fe3−S5	90.13(4)	S1−Ni1−S4	94.01(4)
		11	
Fe1−S1	2.310(3)	Fe1−S3	2.237(2)
Fe2−S3	2.262(3)	Ni1−P2	2.175(2)
Fe1−Fe2	2.6130(19)	Ni1−P1	2.181(2)
Fe3−S4	2.243(3)	Ni1−S2	2.238(2)
S3−Fe1−S1	79.87(9)	S4−Fe4−Fe3	54.02(7)
S3−Fe1−Fe2	54.95(7)	P2−Ni1−P1	86.88(9)
S1−Fe1−Fe2	75.97(8)	P2−Ni1−S2	176.84(10)
S3−Fe2−Fe1	54.05(7)	P1−Ni1−S2	92.78(9)
S4−Fe3−Fe4	54.75(7)	P2−Ni1−S12	91.71(9)

Synthesis and Characterization of Macrocyclic Ni-Bridged Macrocyclic Quadruple-Butterfly Fe/S Clusters [{μ-S(CH$_2$)$_4$-μ}{(μ-S=CS)Fe$_2$(CO)$_6$}$_2$]$_2$[Ni(diphosphine)]$_2$ [diphosphine = dppv (10), dppe (11), dppb (12)]. More interestingly, another type of metallomacrocyclic Ni/Fe/S complex (which contains four butterfly Fe/S cluster units) was found to be prepared by sequential reactions of the $[Et_3NH]^+$ salt of two-μ-CO-containing dianion $[\{\mu\text{-S(CH}_2)_3\text{S-}\mu\}\{(\mu\text{-CO})\text{Fe}_2(\text{CO})_6\}_2]^{2-}$ (**C**; generated in situ from $Fe_3(CO)_{12}$, dithiol $HS(CH_2)_3SH$, and Et_3N) with excess CS_2 and subsequent treatment of the resulting $[Et_3NH]^+$ salt of the two-μ-CS_2-containing dianion $[\{\mu\text{-S(CH}_2)_3\text{S-}\mu\}\{(\mu\text{-S=CS})\text{Fe}_2(\text{CO})_6\}_2]^{2-}$ (**C′**) with dppv-, dppe-, and dppb-chelated $NiCl_2$, respectively (Scheme 3).

It should be noted that, although the two-μ-CO- and two-μ-CS_2-containing dianions **B** and **B′** are known,[19] their analogues **C** and **C′** (which contain a shorter carbon chain than **B** and **B′**) are new. Now, the question is, how were the [2 + 2] type of macrocycles **10−12** generated from dianion **C′** and how were the [1 + 1] type of macrocycles **7−9** produced from similar dianion **B′**? In order to answer these two questions, a possible pathway is proposed (Scheme 4). As shown in Scheme 4, the formation of the [1 + 1] type of macrocycles **7−9** is first via the intermolecular nucleophilic attack of the one negatively charged S atom in dianion **B′** at the Ni atom in (diphosphine)$NiCl_2$ to give intermediate **M$_1$** and then via the intramolecular nucleophilic attack of another negatively charged S atom in **M$_1$** at its Ni atom, followed by ring closure. However, in contrast to intermediate **M$_1$**, the intermediate **M$_2$** [generated similarly by the intermolecular nucleophilic attack of dianion **C′** at the Ni atom of (diphosphine)$NiCl_2$] has difficulty undergoing intramolecular ring closure to give the corresponding [1 + 1] type of macrocycles (presumably because of their high strain caused by the shorter carbon chain in **M$_2$**). So, the [2 + 2] type of macrocycles **10−12** are produced by doubly intermolecular nucleophilic attacks of the two negatively charged S atoms in two molecules of **M$_2$** at their two Ni atoms, respectively. In fact, the suggested pathway described above is not unusual, which is very similar to that previously reported for reactions of dianion **B′** and its analogues with organic dihalides to give the corresponding macrocycles.[19]

The novel [2 + 2] type of macrocycles **10−12** have been fully characterized by elemental analysis and IR and ^{1}H and ^{31}P NMR spectroscopies and, in particular for macrocycle **11**, by X-ray crystallography. Similar to the linear Ni/Fe/S complexes **1−6** and the [1 + 1] type of macrocyclic Ni/Fe/S complexes **7−9**, the IR spectra of **10−12** displayed three absorption bands in the range 2052−1977 cm^{-1} for their terminal CO′s and one medium absorption band in the region 985−983 cm^{-1} for their bridged C=S functional groups.[27−29] In addition, the ^{1}H NMR spectra of **10−12** showed the corresponding signals for their organic groups, whereas their ^{31}P NMR spectra exhibited one singlet at 50.06−60.50 ppm for their diphosphine P atoms. Fortunately, the molecular structure of **11** was further confirmed by X-ray crystallography. Its molecular structure is shown in Figure 7, whereas the selected bond lengths and angles are given in Table 2. As can be seen in Figure 7, complex **11** is another type of Ni/Fe/S macrocyclic complex, which includes four single-butterfly Fe/S cluster moieties. The four cluster moieties Fe1Fe2S3S1C7S2, Fe3Fe4S4S5C17S6, Fe5Fe6S9S8C18S7, and Fe7Fe8S10S11C34S12 are connected by two propylene chains (via S3/S4 and S9/S10) and two dppe-chelated Ni1 and Ni2 atoms (via S2/S12 and S6/S7) to give a 32-membered metallomacrocycle Ni1S2C7S1Fe1Fe2S3C8C9C10S4Fe4Fe3S5C17S6Ni2S7C18S8Fe6Fe5S9C25C26C27S10Fe7Fe8S11C34S12. It is noteworthy that the propylene group, in contrast to the butylene group in **8**, is attached to S3/S4 and S9/S10 in equatorial positions[30,31] (nonbonded angles: ∠C10−S4···S5 = 162.37°, ∠C8−S3···S1 = 164.51°, ∠C25−S9···S8 = 163.85°, and ∠C27−S10···S11 = 160.65°) because it is the [2 + 2] type of macrocycle that is much larger than the [1 + 1] type of macrocycle **8**. In addition, similar to macrocycle **8**, the Fe atoms of **11** adopt the square-pyramidal geometry with normal Fe−Fe bond lengths (average value: 2.625 Å),[19,33,34] and the Ni atoms have the slightly distorted square-planar geometry with normal Ni−S (average value: 2.241 Å) and Ni−P (average value: 2.184 Å) bond lengths.[35−37]

Scheme 3

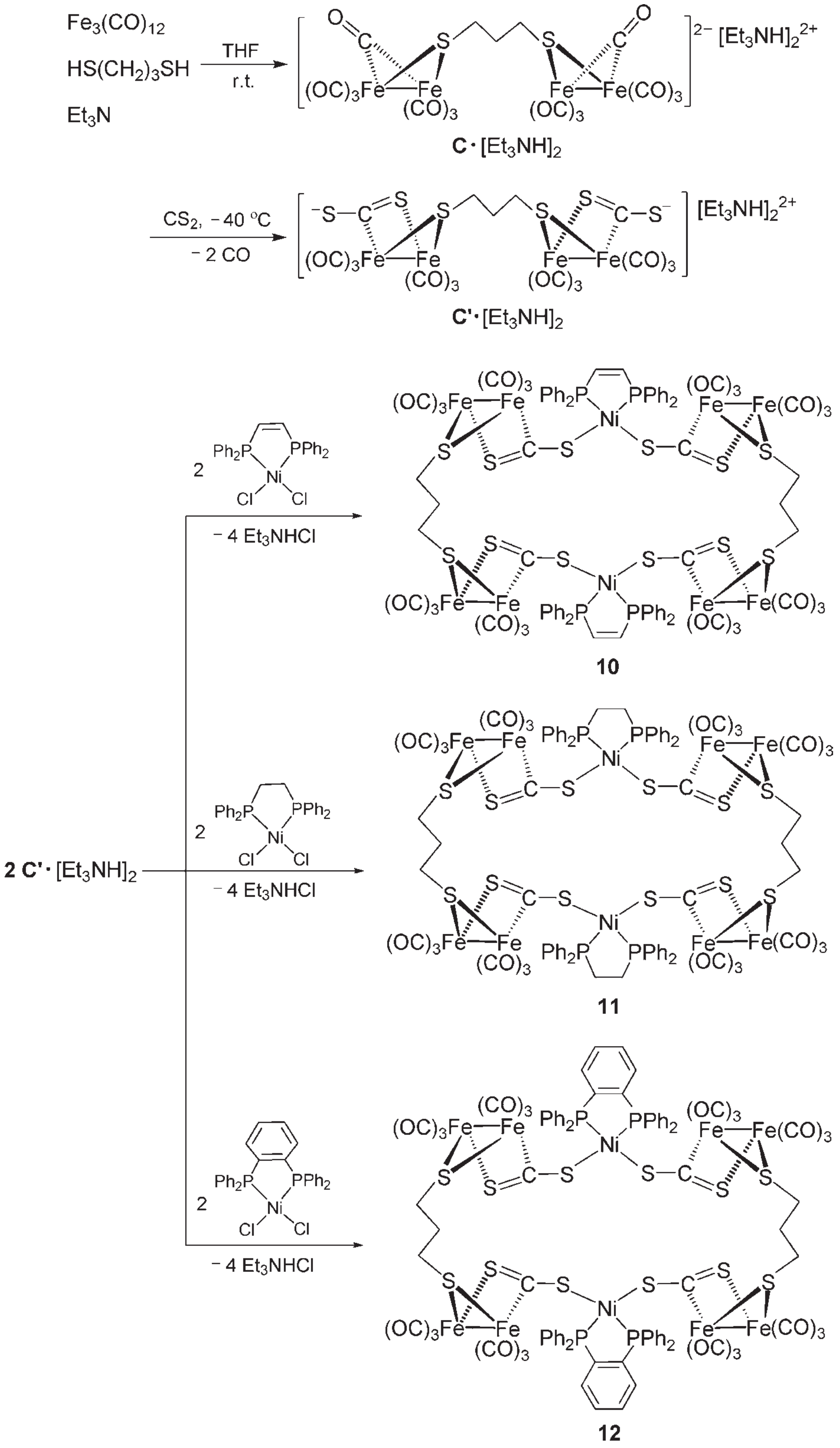

Conclusions

We have synthesized three series of the new Ni/Fe/S complexes **1**−**12** successfully. The linear type of Ni/Fe/S complexes **1**−**6** were prepared by sequential reactions involving the final step reaction of monoanions **A**′ with (diphosphine)NiCl$_2$, while the two types of macrocyclic Ni/Fe/S complexes **7**−**9** and **10**−**12** were prepared by sequential reactions involving the final step reaction of dianions **B**′ and **C**′ with (diphosphine)NiCl$_2$, respectively. Interestingly, it is the carbon chain length present in **B**′ and **C**′ that decided the formation of the two different types of metallomacrocycles **7**−**9** and **10**−**12**. While a possible pathway is suggested for production of the two types of macrocycles, the crystal structures of the representatives of the three types of complexes,

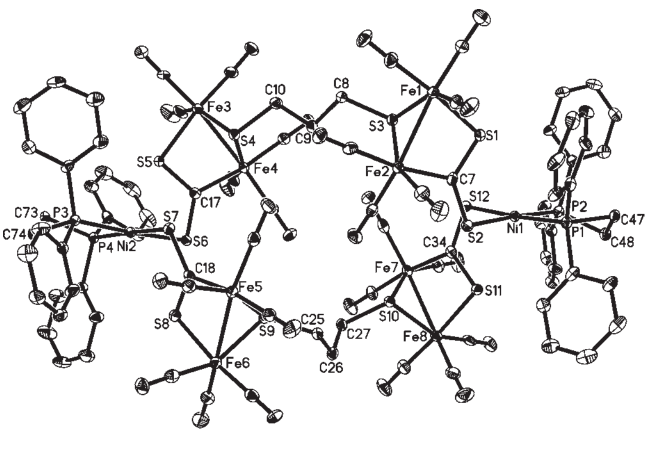

Figure 7. ORTEP view of **11** with 30% probability level ellipsoids.

Scheme 4

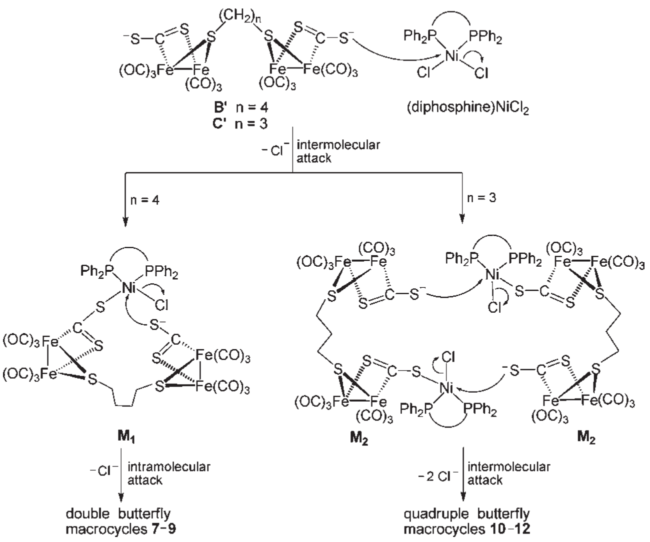

namely, **1**, **2**, **4**, **5**, **8**, and **11**, were determined by X-ray crystallography. Further studies on reactions of the Se analogues of dianions **B**/**B′** and **C**/**C′** to make the corresponding macrocyclic Ni/Fe/E (E = S, Se) complexes will be carried out in this laboratory.

Experimental Section

General Comments. All reactions were carried out using standard Schlenk and vacuum-line techniques under a N_2 atmosphere. Tetrahysrofuran (THF) was purified by distillation from sodium/benzophenone ketyl. RSH (R = Et, *n*-Bu, *t*-Bu, Ph), $HS(CH_2)_nSH$ (*n* = 3, 4), and some other materials were available commercially and used as received. $Fe_3(CO)_{12}$,[38] Ni(dppv)-Cl_2 (dppv = $Ph_2PCH{=}CHPPh_2$),[39] Ni(dppe)Cl_2 (dppe = $Ph_2PCH_2CH_2PPh_2$),[39] and Ni(dppb)Cl_2 [dppb = 1,2-$(Ph_2P)_2C_6H_4$][40] were prepared according to literature procedures. Preparative thin-layer chromatography (TLC) was carried out on glass plates (26 × 20 × 0.25 cm) coated with silica gel H (10−40 μm). IR spectra were recorded on a Bruker Vector 22 IR spectrophotometer. ^1H (^{31}P) NMR spectra were obtained on a Varian Mercury Plus 400 NMR spectrometer. Elemental analyses were performed on an Elementar Vario EL analyzer. Melting points were determined on a SGW X-4 microscopic melting point apparatus and were uncorrected.

Preparation of [(μ-EtS)(μ-S=CS)$Fe_2(CO)_6]_2$[Ni(dppv)] (1). A 100 mL three-necked flask equipped with a magnetic stir bar, a rubber septum, and a nitrogen inlet tube was charged with EtSH (0.074 mL, 1.0 mmol), $Fe_3(CO)_{12}$ (0.504 g, 1.0 mmol), Et_3N (0.140 mL, 1.0 mmol), and THF (15 mL). The mixture was stirred at room temperature for 0.5 h to give a brown-red solution containing monoanion $[(\mu\text{-EtS})(\mu\text{-CO})Fe_2(CO)_6]^-$.[24,25] The solution was cooled to −40 °C, and then CS_2 (0.120 mL, 2.0 mmol) was added. The new mixture containing monoanion $[(\mu\text{-EtS})(\mu\text{-SC{=}S})Fe_2(CO)_6]^-$[26,27] was allowed to warm to room temperature and stirred at this temperature for 0.5 h. After Ni(dppv)Cl_2 (0.263 g, 0.5 mmol) was added, the new mixture was stirred for 2 h. The solvent was removed at reduced pressure, and the residue was subjected to TLC separation using CH_2Cl_2/petroleum ether (1:2, v/v) as the eluent. From the main red band, complex **1** (0.412 g, 64%) was obtained as a red solid. Mp: 85 °C (dec). Anal. Calcd for $C_{44}H_{32}Fe_4NiO_{12}P_2S_6$: C, 41.00; H, 2.50. Found: C, 40.90; H, 2.75. IR (KBr disk): $\nu_{C\equiv O}$ 2053 (s), 2015 (vs), 1976 (vs); $\nu_{C=S}$ 986 (m) cm^{-1}. ^1H NMR (400 MHz, $CDCl_3$): 1.41 (t, *J* = 7.0 Hz, 6H, $2CH_3$), 2.37 (q, *J* = 6.8 Hz, 2H, a-CH_2), 2.58 (q, *J* = 6.0 Hz, 2H, e-CH_2), 6.80−7.06 (m, 2H, CH=CH), 7.30−7.61 (m, 20H, $4C_6H_5$) ppm. ^{31}P NMR (162 MHz, $CDCl_3$, 85% H_3PO_4): 61.83 (s) ppm.

Preparation of [(μ-*t*-BuS)(μ-S=CS)$Fe_2(CO)_6]_2$[Ni(dppv)] (2). The same procedure as that for **1** was followed, but *t*-BuSH (0.112 mL, 1.0 mmol) was used instead of EtSH. From the main red band, complex **2** (0.346 g, 52%) was obtained as a red solid. Mp: 91 °C (dec). Anal. Calcd for $C_{48}H_{40}Fe_4NiO_{12}P_2S_6$: C, 42.86; H, 3.00. Found: C, 42.65; H, 2.95. IR (KBr disk): $\nu_{C\equiv O}$ 2050 (s), 2014 (vs), 1974 (vs); $\nu_{C=S}$ 986 (m) cm^{-1}. ^1H NMR (400 MHz, $CDCl_3$): 1.42 (s, 18H, $2C(CH_3)_3$), 6.78−7.05 (m, 2H, CH=CH), 7.34−7.59 (m, 20H, $4C_6H_5$) ppm. ^{31}P NMR (162 MHz, $CDCl_3$, 85% H_3PO_4): 61.60 (s) ppm.

Preparation of [(μ-*n*-BuS)(μ-S=CS)$Fe_2(CO)_6]_2$[Ni(dppe)] (3). The same procedure as that for **1** was followed, but *n*-BuSH (0.108 mL, 1.0 mmol) and Ni(dppe)Cl_2 (0.264 g, 0.5 mmol) were utilized in place of EtSH and Ni(dppv)Cl_2, respectively. From the main red band, complex **3** (0.497 g, 74%) was obtained as a red solid. Mp: 84 °C (dec). Anal. Calcd for $C_{48}H_{42}Fe_4O_{12}NiP_2S_6$: C, 42.79; H, 3.14. Found: C, 42.78; H, 3.24. IR (KBr disk): $\nu_{C\equiv O}$ 2053 (s), 2014 (vs), 1975 (vs); $\nu_{C=S}$ 987 (m) cm^{-1}. ^1H NMR (400 MHz, $CDCl_3$): 0.97 (br s, 6H, $2CH_3$), 1.51 (s, 4H, $2CH_2CH_3$), 1.73 (s, 4H, $2CH_2CH_2CH_3$), 2.10−2.63 (m, 8H, $2SCH_2$, PCH_2CH_2P), 7.28−7.70 (m, 20H, $4C_6H_5$) ppm. ^{31}P NMR (162 MHz, $CDCl_3$, 85% H_3PO_4): 51.62 (s) ppm.

Preparation of [(μ-PhS)(μ-S=CS)$Fe_2(CO)_6]_2$[Ni(dppe)] (4). The same procedure as that for **1** was followed, but PhSH (0.110 mL, 1.0 mmol) and Ni(dppe)Cl_2 (0.264 g, 0.5 mmol) were used in place of EtSH and Ni(dppv)Cl_2, respectively. From the main red band, complex **4** (0.419 g, 60%) was obtained as a red solid. Mp: 96 °C (dec). Anal. Calcd for $C_{52}H_{34}Fe_4O_{12}NiP_2S_6$: C, 45.02; H, 2.47. Found: C, 45.17; H, 2.55. IR (KBr disk): $\nu_{C\equiv O}$ 2057 (s), 2018 (vs), 1979 (vs); $\nu_{C=S}$ 989 (m) cm^{-1}. ^1H NMR (400 MHz, $CDCl_3$): 2.20 (br s, 4H, $2CH_2$), 7.15−7.54 (m, 30H, $6C_6H_5$) ppm. ^{31}P NMR (162 MHz, $CDCl_3$, 85% H_3PO_4): 52.14 (s) ppm.

Preparation of [(μ-EtS)(μ-S=CS)$Fe_2(CO)_6]_2$[Ni(dppb)] (5). The same procedure as that for **1** was followed, but Ni(dppb)Cl_2 (0.288 g, 0.5 mmol) was employed in place of Ni(dppv)Cl_2. From the main red band, complex **5** (0.410 g, 61%) was obtained as a red solid. Mp: 92 °C (dec). Anal. Calcd for $C_{48}H_{34}Fe_4NiO_{12}P_2S_6$: C, 43.05; H, 2.56. Found: C, 43.17; H, 2.59. IR (KBr disk): $\nu_{C\equiv O}$ 2053 (s), 2014 (vs), 1976 (vs); $\nu_{C=S}$ 984 (m) cm^{-1}. ^1H NMR (400 MHz, $CDCl_3$): 1.41 (t, *J* = 6.8 Hz, 6H, $2CH_3$), 2.39 (q, *J* = 7.6 Hz, 2H, a-CH_2), 2.58 (q, *J* = 6.4 Hz, 2H, e-CH_2), 7.39−7.51

---

[38] King, R. B. Transition-Metal Compounds. *Organometallic Syntheses*; Academic Press: New York, 1965; Vol. *I*, p 95.

[39] Bomfim, J. A. S.; de Souza, F. P.; Filgueiras, C. A. L.; de Sousa, A. G.; Gambardella, M. T. P. *Polyhedron* **2003**, *22*, 1567.

[40] Gray, L. R.; Higgins, S. J.; Levason, W.; Webster, M. *J. Chem. Soc., Dalton. Trans.* **1984**, 459.

(m, 24H, $4C_6H_5$, C_6H_4) ppm. ^{31}P NMR (162 MHz, $CDCl_3$, 85% H_3PO_4): 54.93 (s) ppm.

Preparation of [(μ-*t*-BuS)(μ-S=CS)$Fe_2(CO)_6$]$_2$[Ni(dppb)] (6). The same procedure as that for **1** was followed, but *t*-BuSH (0.112 mL, 1.0 mmol) and Ni(dppb)Cl_2 (0.288 g, 0.5 mmol) were used in place of EtSH and Ni(dppv)Cl_2, respectively. From the main red band, complex **6** (0.424 g, 61%) was obtained as a red solid. Mp: 93 °C (dec). Anal. Calcd for $C_{52}H_{42}Fe_4NiO_{12}P_2S_6$: C, 44.76; H, 3.03. Found: C, 44.55; H, 3.26. IR (KBr disk): $\nu_{C\equiv O}$ 2050 (s), 2013 (vs), 1974 (vs); $\nu_{C=S}$ 986 (m) cm^{-1}. ^{1}H NMR (400 MHz, $CDCl_3$): 1.43 (s, 18H, $2C(CH_3)_3$), 7.30−7.65 (m, 24H, $4C_6H_5$, C_6H_4) ppm. ^{31}P NMR (162 MHz, $CDCl_3$, 85% H_3PO_4): 55.65 (s) ppm.

Preparation of [μ-S(CH_2)$_4$S-μ][(μ-S=CS)$Fe_2(CO)_6$]$_2$[Ni(dppv)] (7). The same equipped flask as that for the preparation of **1** was charged with $HS(CH_2)_4SH$ (0.062 mL, 0.5 mmol), $Fe_3(CO)_{12}$ (0.504 g, 1.0 mmol), Et_3N (0.140 mL, 1.0 mmol), and THF (15 mL). The mixture was stirred at room temperature for 0.5 h to give a brown-red solution containing the dianion[19] [{μ-S(CH_2)$_4$S-μ}{(μ-CO)$Fe_2(CO)_6$}$_2$]$^{2-}$. The solution was cooled to −40 °C, and then CS_2 (0.120 mL, 2.0 mmol) was added. The new mixture containing the dianion[19] [{μ-S(CH_2)$_4$S-μ}{(μ-SC=S)-$Fe_2(CO)_6$}$_2$]$^{2-}$ was allowed to warm to room temperature and stirred at this temperature for 0.5 h. After Ni(dppv)Cl_2 (0.263 g, 0.5 mmol) was added, the new mixture was stirred for an additional 12 h. The solvent was removed at reduced pressure, and the residue was subjected to TLC using CH_2Cl_2/petroleum ether (2:3, v/v) as the eluent. From the main red band, complex **7** (0.095 g, 15%) was obtained as a red solid. Mp: 120 °C (dec). Anal. Calcd for $C_{44}H_{30}Fe_4NiO_{12}P_2S_6$: C, 41.06; H, 2.35. Found: C, 41.24; H, 2.60. IR (KBr disk): $\nu_{C\equiv O}$ 2053 (s), 2015 (vs), 1976 (vs); $\nu_{C=S}$ 991 (m) cm^{-1}. ^{1}H NMR (400 MHz, $CDCl_3$): 1.86−2.84 (m, 8H, $4CH_2$), 6.74−6.96 (m, 2H, CH=CH), 7.42−7.69 (m, 20H, $4C_6H_5$) ppm. ^{31}P NMR (162 MHz, $CDCl_3$, 85% H_3PO_4): 62.45 (s) ppm.

Preparation of [μ-S(CH_2)$_4$S-μ][(μ-S=CS)$Fe_2(CO)_6$]$_2$[Ni(dppe)] (8). The same procedure as that for **7** was followed, but Ni(dppe)Cl_2 (0.264 g, 0.5 mmol) was used instead of Ni(dppv)Cl_2. From the main red band, complex **8** (0.100 g, 16%) was obtained as a red solid. Mp: 125 °C (dec). Anal. Calcd for $C_{44}H_{32}Fe_4NiO_{12}P_2S_6$: C, 40.99; H, 2.50. Found: C, 41.05; H, 2.76. IR (KBr disk): $\nu_{C\equiv O}$ 2053 (s), 2015 (s), 1976 (vs); $\nu_{C=S}$ 990 (m) cm^{-1}. ^{1}H NMR (400 MHz, $CDCl_3$): 1.88−2.85 (m, 12H, $6CH_2$) 7.45−7.75 (m, 20H, $4C_6H_5$) ppm. ^{31}P NMR (162 MHz, $CDCl_3$, 85% H_3PO_4): 53.79 (s) ppm.

Preparation of [μ-S(CH_2)$_4$S-μ][(μ-S=CS)$Fe_2(CO)_6$]$_2$[Ni(dppb)] (9). The same procedure as that for **7** was followed, but Ni(dppb)Cl_2 (0.288 g, 0.5 mmol) was employed in place of Ni(dppv)Cl_2. From the main red band, complex **9** (0.104 g, 16%) was obtained as a red solid. Mp: 114 °C (dec). Anal. Calcd for $C_{48}H_{32}Fe_4NiO_{12}P_2S_6$: C, 43.11; H, 2.41. Found: C, 42.85; H, 2.70. IR (KBr disk): $\nu_{C\equiv O}$ 2053 (vs), 2015 (vs), 1975 (vs); $\nu_{C=S}$ 989 (m) cm^{-1}. ^{1}H NMR (400 MHz, $CDCl_3$): 1.80−2.84 (m, 8H, $4CH_2$), 7.29−7.63 (m, 24H, $4C_6H_5$, C_6H_4) ppm. ^{31}P NMR (162 MHz, $CDCl_3$, 85% H_3PO_4): 54.81 (s) ppm.

Preparation of [{μ-S(CH_2)$_3$S-μ}{(μ-S=CS)$Fe_2(CO)_6$}$_2$]$_2$[Ni(dppv)]$_2$ (10). The same equipped flask as that for the preparation of **1** was charged with $HS(CH_2)_3SH$ (0.050 mL, 0.5 mmol), $Fe_3(CO)_{12}$ (0.504 g, 1.0 mmol), Et_3N (0.140 mL, 1.0 mmol), and THF (15 mL). The mixture was stirred at room temperature for 0.5 h to give a brown-red solution containing dianion [{μ-S(CH_2)$_3$S-μ}{(μ-CO)$Fe_2(CO)_6$}$_2$]$^{2-}$. After the solution was cooled to −40 °C, CS_2 (0.120 mL, 2.0 mmol) was added. The new mixture containing dianion [{μ-S(CH_2)$_3$S-μ}{(μ-SC=S)$Fe_2(CO)_6$}$_2$]$^{2-}$ was allowed to warm to room temperature and stirred at this temperature for 0.5 h. After Ni(dppv)Cl_2 (0.263 g, 0.5 mmol) was added, the new mixture was stirred for an additional 12 h. The solvent was removed at reduced pressure, and then the residue was subjected to TLC using CH_2Cl_2/petroleum ether (2:3, v/v) as the eluent. From the main red band, complex **10** (0.135 g, 21%) was obtained as a red solid. Mp: 95 °C (dec). Anal. Calcd for $C_{86}H_{56}Fe_8Ni_2O_{24}P_4S_{12}$: C, 40.57; H, 2.22. Found: C, 40.51; H, 2.35. IR (KBr disk): $\nu_{C\equiv O}$ 2052 (s), 2013 (vs), 1978 (vs); $\nu_{C=S}$ 983 (m) cm^{-1}. ^{1}H NMR (400 MHz, $CDCl_3$): 2.00−2.65 (m, 12H, $6CH_2$), 6.72−7.00 (m, 4H, 2CH=CH), 7.27−7.59 (m, 40H, $8C_6H_5$) ppm. ^{31}P NMR (162 MHz, $CDCl_3$, 85% H_3PO_4): 60.50 (s) ppm.

Preparation of [{μ-S(CH_2)$_3$S-μ}{(μ-S=CS)$Fe_2(CO)_6$}$_2$]$_2$[Ni(dppe)]$_2$ (11). The same procedure as that for **10** was followed, but Ni(dppe)Cl_2 (0.264 g, 0.5 mmol) was used instead of Ni(dppv)Cl_2. From the main red band, complex **11** (0.140 g, 22%) was obtained as a red solid. Mp: 90 °C (dec). Anal. Calcd for

Table 3. Crystal Data and Structure Refinements Details for **1**, **2**, **4**, and **5**

	1	2	4	5
mol formula	$C_{44}H_{32}Fe_4NiO_{12}$-$P_2S_6\cdot 1.5CHCl_3$	$C_{48}H_{40}Fe_4NiO_{12}$-$P_2S_6\cdot 0.5C_6H_{14}$	$C_{52}H_{34}Fe_4NiO_{12}$-$P_2S_6\cdot 0.25CH_2Cl_2$	$C_{48}H_{34}Fe_4NiO_{12}$-$P_2S_6\cdot CH_2Cl_2$
mol wt	1468.16	1388.30	1408.43	1424.09
cryst syst	monoclinic	triclinic	monoclinic	triclinic
space group	*C*2/*c*	$P\bar{1}$	*C*2/*c*	$P\bar{1}$
a/Å	20.511(4)	11.6271(3)	35.014(7)	13.768(2)
b/Å	18.674(4)	15.4929(9)	14.720(3)	13.877(2)
c/Å	30.382(6)	18.9112(12)	27.319(6)	15.743(3)
α/deg	90	101.097(9)	90	98.289(6)
β/deg	98.52(3)	103.997(15)	124.11(3)	102.325(12)
γ/deg	90	108.164(6)	90	92.974(9)
V/Å^3	11508(4)	3005.3(10)	11658(4)	2897.2(8)
Z	8	2	8	2
D_c/g cm^{-3}	1.695	1.534	1.605	1.632
abs coeff/mm^{-1}	1.844	1.567	1.640	1.717
F(000)	5896	1414	5684	1436
index ranges	$-23 \le h \le 24$ $-22 \le k \le 21$ $-36 \le l \le 26$	$-14 \le h \le 14$ $-19 \le k \le 15$ $-23 \le l \le 23$	$-41 \le h \le 39$ $-17 \le k \le 17$ $-32 \le l \le 32$	$-17 \le h \le 14$ $-17 \le k \le 15$ $-19 \le l \le 20$
no. of reflns	38 169	22 185	43 162	19 292
no. of indep reflns	10 158	11 649	10 301	12 553
$2\theta_{max}$ /deg	50.04	50.04	50.04	50.04
R	0.0475	0.0755	0.0576	0.0569
R_w	0.1238	0.1699	0.1607	0.1368
GOF	1.068	1.027	1.102	1.049
largest diff peak and hole/e Å^{-3}	1.380/−1.140	1.279/−1.078	1.536/−0.752	1.420/−0.917

Table 4. Crystal Data and Structure Refinements Details for **8** and **11**

	8	**11**
mol formula	$C_{44}H_{32}Fe_4NiO_{12}P_2S_6 \cdot CH_2Cl_2$	$C_{86}H_{60}Fe_8Ni_2O_{24}P_4S_{12} \cdot 0.25CH_2Cl_2 \cdot C_6H_{14} \cdot 4.5CHCl_3$
mol wt	1374.03	3191.57
cryst syst	triclinic	monoclinic
space group	$P\bar{1}$	$P2(1)/c$
a/Å	12.002(2)	28.397(6)
b/Å	12.612(3)	18.564(4)
c/Å	18.554(4)	27.180(5)
α/deg	84.05(3)	90
β/deg	80.08(3)	115.36(3)
γ/deg	70.43(3)	90
V/Å^3	2603.5(9)	12947(4)
Z	2	4
D_c/g cm^{-3}	1.753	1.637
abs coeff/mm^{-1}	1.907	1.751
F(000)	1384	6415
index ranges	$-13 \leq h \leq 14$ $-13 \leq k \leq 15$ $-22 \leq l \leq 22$	$-23 \leq h \leq 33$ $-21 \leq k \leq 22$ $-32 \leq l \leq 30$
no. of reflns	20 770	86 061
no. of indep reflns	9134	22 845
$2\theta_{max}$ /deg	50.04	50.04
R	0.0370	0.0865
R_w	0.0764	0.2348
GOF	1.007	1.105
largest diff peak and hole/e Å^{-3}	0.388/−0.671	2.000/−1.347

$C_{86}H_{60}Fe_8Ni_2O_{24}P_4S_{12}$: C, 40.50; H, 2.37. Found: C, 40.31; H, 2.51. IR (KBr disk): $\nu_{C\equiv O}$ 2052 (s), 2013 (vs), 1977 (vs); $\nu_{C=S}$ 985 (m) cm^{-1}. ^{1}H NMR (400 MHz, $CDCl_3$): 1.96−2.64 (m, 20H, 10CH_2), 7.17−7.75 (m, 40H, 8C_6H_5) ppm. ^{31}P NMR (162 MHz, $CDCl_3$, 85% H_3PO_4): 50.06 (s) ppm.

Preparation of [{μ-S(CH_2)$_3$S-μ}{(μ-S=CS)Fe_2(CO)$_6$}$_2$]$_2$[Ni(dppb)]$_2$ (12). The same procedure as that for **10** was followed, but Ni(dppb)Cl_2 (0.288 g, 0.5 mmol) was utilized instead of Ni(dppv)Cl_2. From the main red band, complex **12** (0.150 g, 23%) was obtained as a red solid. Mp: 94 °C (dec). Anal. Calcd for $C_{94}H_{60}Fe_8Ni_2O_{24}P_4S_{12}$: C, 42.67; H, 2.29. Found: C, 42.44; H, 2.30. IR (KBr disk): $\nu_{C\equiv O}$ 2052 (s), 2013 (vs), 1977 (vs); $\nu_{C=S}$ 984 (m) cm^{-1}. ^{1}H NMR (400 MHz, $CDCl_3$): 2.02−2.63 (m, 12H, 6CH_2), 7.34−7.46 (m, 48H, 8C_6H_5, 2C_6H_4) ppm. ^{31}P NMR (162 MHz, $CDCl_3$, 85% H_3PO_4): 53.73 (s) ppm.

X-ray Structure Determinations of 1, 2, 4, 5, 8, and 11. The single crystals suitable for X-ray diffraction analyses were grown by the slow evaporation of $CHCl_3$/n-hexane solutions of **1** and **11** or CH_2Cl_2/n-hexane solutions of **2**, **4**, **5**, and **8** at about −10 °C. All of the single crystals were mounted on a Rigaku MM-007 (rotating-anode) diffractometer equipped with a Saturn 70 CCD. Data were collected at 113 K by using a graphite monochromator with Mo Kα radiation (λ = 0.710 73 or 0.710 75 Å) in the ω−ϕ scanning mode. Absorption correction was performed by the *CrystalClear* program.[41] The structures were solved by direct methods using the *SHELXS-97* program[42] and refined by full-matrix least-squares techniques (*SHELXL-97*)[43] on F^2. H atoms were located by using the geometric method. Details of the crystal data, data collections, and structure refinements are summarized in Tables 3 and 4.

Acknowledgment. We are grateful to the National Natural Science Foundation of China (Grants 20772059 and 20972073) and the Tianjin Natural Science Foundation (Grant 09JCZDJC27900) for financial support.

Supporting Information Available: Full tables of crystal data, atomic coordinates and thermal parameters, and bond lengths and angles for **1**, **2**, **4**, **5**, **8**, and **11** as CIF files. This material is available free of charge via the Internet at http://pubs.acs.org.

---

(41) *CrystalClear and Crystalstructure*; Rigaku and Rigaku Americas: The Woodlands, TX.

(42) Sheldrick, G. M. *SHELXS97, A Program for Crystal Structure Solution*; University of Göttingen: Göttingen, Germany, 1997.

(43) Sheldrick, G. M. *SHELXL97, A Program for Crystal Structure Refinement*; University of Göttingen: Göttingen, Germany, 1997.